Monitoring calcium-induced conformational changes in recoverin by electrospray mass spectrometry

ARTICLE *in* PROTEIN SCIENCE · APRIL 2008

Impact Factor: 2.85 · DOI: 10.1002/pro.5560060411 · Source: PubMed

Protein Science (1997), *6*:843–850. Cambridge University Press. Printed in the USA.

Monitoring calcium-induced conformational changes in recoverin by electrospray mass spectrometry

THOMAS A. NEUBERT,[1,2,3] KENNETH A. WALSH,[1] JAMES B. HURLEY,[1,2] AND RICHARD S. JOHNSON[1]

[1]Department of Biochemistry, University of Washington, Seattle, Washington 98195
[2]Howard Hughes Medical Institute, University of Washington, Seattle, Washington 98195

(RECEIVED September 30, 1996; ACCEPTED January 2, 1997)

Abstract

Recoverin is a calcium-binding protein that regulates the vertebrate photoresponse by inhibiting rhodopsin kinase in response to high calcium concentrations. It is heterogeneously N-acylated by myristoyl and related fatty acyl residues that are thought to act as "calcium-myristoyl switches," whereby, in the presence of Ca^{2+}, the N-terminal acyl group is extended away from recoverin and, in the absence of calcium, it is more closely associated with the protein. Here we use electrospray ionization mass spectrometry (ESI/MS) to examine hydrogen isotopic exchange rates for specific regions of both acylated and nonacylated recoverin in the presence and absence of calcium. The deuterium exchange rates of three regions in the hydrophobic myristoyl binding pocket of acylated recoverin decreased in the absence of calcium. This effect is most likely due to the closer association of the acyl group with the protein under these conditions. In contrast, rates of deuterium incorporation increased in the absence of calcium for other regions, including the two functional calcium-binding sites. In addition to supporting the calcium-myristoyl switch hypothesis, a comparison of the behavior of acylated and unacylated recoverin revealed that the N-acyl group (N-lauroyl or N-myristoyl) exerts a significant stabilizing influence on the dynamics of recoverin. We demonstrate that the new technique of monitoring hydrogen isotopic exchange by ESI/MS can be used to obtain useful information concerning protein structures in solution using smaller amounts of protein and under more physiologically relevant conditions than is typically possible with NMR or X-ray crystallography.

Keywords: calcium-binding; hydrogen isotope exchange; mass spectrometry; N-acylation; protein dynamics; recoverin

Recoverin is a Ca^{2+}-binding protein involved in visual signal transduction. It is thought to regulate the duration of the photoresponse (Gray-Keller et al., 1993) by regulating rhodopsin phosphorylation (Kawamura, 1993) via Ca^{2+}-dependent inhibition of rhodopsin kinase (Chen et al., 1995). The N-terminal glycine of recoverin is modified by a family of fatty acyl groups (Dizhoor et al., 1992) that influences recoverin activity (Sanada et al., 1995). It has been proposed that this protein contains a "calcium-myristoyl switch," whereby Ca^{2+} binding to recoverin induces extension of the acyl group, thereby allowing it to interact with membranes and/or other proteins. In the absence of Ca^{2+}, the acyl group is thought to be associated more closely with recoverin (Zozulya & Stryer, 1992; Dizhoor et al., 1993).

We have used the new technique of monitoring rates of HDX by mass spectrometry (Katta & Chait, 1993; Zhang & Smith, 1993; Johnson & Walsh, 1994) to compare the structures of both acylated and nonacylated recoverin in the calcium-bound and calcium-free states. With this method, the protein of interest is incubated under various experimental conditions in the presence of buffer containing deuterated water. The deuterium exchange reaction is quenched by dropping both the temperature and pH, the protein is cleaved by an acid protease, and the degree of HDX that took place in the regions of the proteins corresponding to the proteolytic fragments is measured by ESI/MS (Fenn et al., 1989). The partially deuterated peptides are desalted and fractionated by LC/MS (Covey et al., 1991). This technique primarily examines isotopic exchange of backbone amide hydrogens, because most side-chain hydrogens are back-exchanged rapidly during the analysis.

The rates of amide hydrogen exchange within folded proteins are known to vary over eight orders of magnitude, and it is thought that reduced rates of exchange correspond to an increase in amide

Reprint requests to Richard S. Johnson at his present address: Immunex Corporation, 51 University Street, Seattle, Washington 98101-2936; e-mail: rjohnson@immunex.com.

[3]Present address: Fournier Pharma GmbH, 104 Waldhofer Strasse, D-69123 Heidelberg, Germany.

Abbreviations: C14:0, myristic acid; C12:0, lauric acid; ESI/MS, electrospray ionization mass spectrometry; HDX, hydrogen/deuterium exchange; LC/MS, liquid chromatography/mass spectrometry.

hydrogen bond stability (Englander & Kallenbach, 1984), and/or reduced accessibility of solvent to amide hydrogens (Woodward et al., 1982). Although this mass spectrometric method provides less structural detail than either NMR or crystallography, it can be used with subnanomolar amounts of material, in dilute aqueous solution, and on large proteins or even protein complexes (Liu & Smith, 1994; Zhang et al., 1996). Here we present mass spectrometric data that supports the calcium-myristoyl switch hypothesis by providing a framework for understanding the differences and similarities between the crystallographic structure of unacylated Ca^{2+} and Sm^{3+}-bound recoverin (Flaherty et al., 1993) and the NMR structure of N-myristoylated unliganded recoverin (Tanaka et al., 1995). In addition, our data provide new information suggesting that either Ca^{2+} binding or N-acylation is needed to stabilize the overall structure of recoverin.

Results

HDX measurements

Figure 1 shows an ESI mass spectrum of a proteolytic (peptic) fragment of recoverin (containing amino acids 85–89) after 180 min of deuterium exchange in the absence (Fig. 1A) or presence (Fig. 1B) of 1 mM Ca^{2+}. It is clear that Ca^{2+} increases the rate of HDX within this segment, and that this change in mass is detected readily.

Figures 2 and 3 represent summaries of such mass analyses for three different peptides derived from unmodified (U) or myristoylated (M) recoverin incubated in the presence (white bars) or absence (black bars) of Ca^{2+} for various lengths of time. HDX is expressed as the percentage of deuterium that had been incorporated within each peptide compared to its fully deuterated control. Figure 2 shows data for two peptides, each derived from one of the calcium-binding helix-loop-helix "EF hands" (Moncrief et al., 1990;

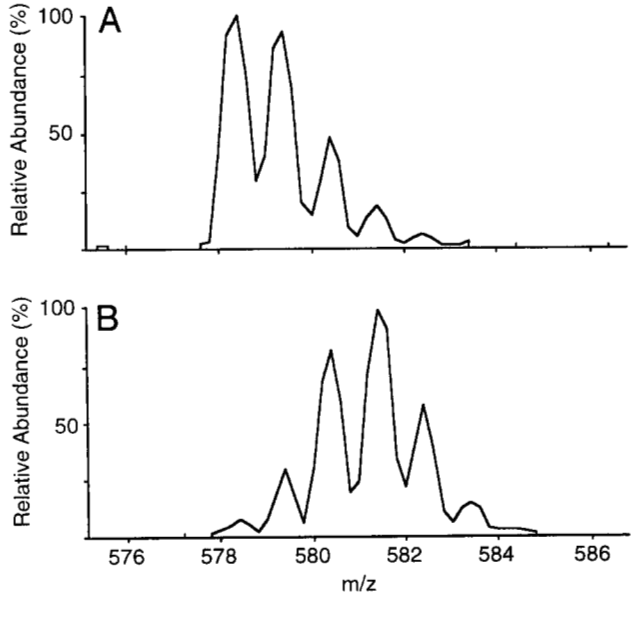

Fig. 1. ESI mass spectra of the $(M + H)^+$ ions of the peptic peptides encompassing residues 85–89 of myristoylated recoverin after incubation in D_2O for 180 min in the (**A**) absence or (**B**) presence of 1 mM Ca^{2+}.

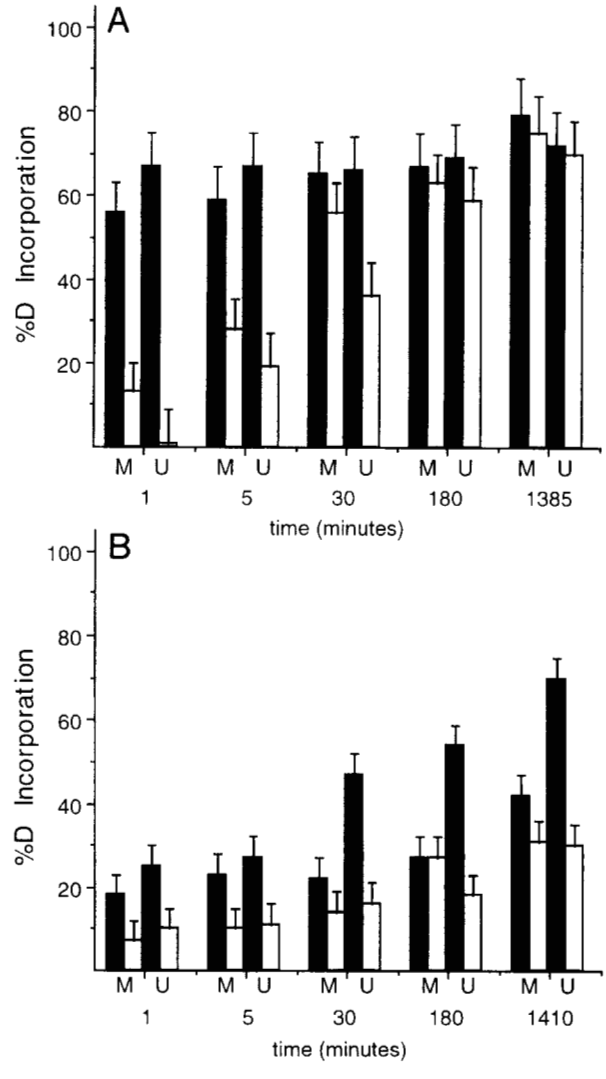

Fig. 2. Regions of EF hand 2 and EF hand 3 of recoverin that are stabilized by calcium ions. Bar plots showing deuterium incorporation after incubation in buffered D_2O (pD 7.4) for various times for regions of myristoylated (M) and unmodified (U) recoverin encompassing residues (**A**) 64–80 and (**B**) 108–122. Residues 64–80 include a portion of the Ca^{2+}-binding loop of EF-hand 2 and residues 108–122 encompass all of the Ca^{2+}-binding loop of EF-hand 3; both were found to exhibit a reduced rate of HDX in the presence (white bars) of 1 mM Ca^{2+} compared to similar treatment without calcium (black bars).

Flaherty et al., 1993) of both myristoylated and unmodified recoverin. In both regions, deuterium exchange is slowed when Ca^{2+} is present during the exchange reaction. This stabilizing effect of Ca^{2+} was more pronounced for unmodified recoverin (see Table 1), especially for peptide 108–122 (Fig. 2B), which contains the Ca^{2+}-binding loop of EF hand 3.

Figure 3 shows data for a region of recoverin (residues 85–89) whose rate of HDX for the myristoylated form is increased nearly 100-fold (Table 1) in the presence of Ca^{2+}, whereas the opposite effect was observed for unmodified recoverin. For comparison, the same region of recoverin (residues 85–89) is shown in Figure 4 for recoverin N-acylated by lauric acid. Again, HDX is increased in the presence of Ca^{2+}, but to a lesser degree than for N-myristoylated recoverin (13-fold versus 85-fold, as shown in Table 2). Similar

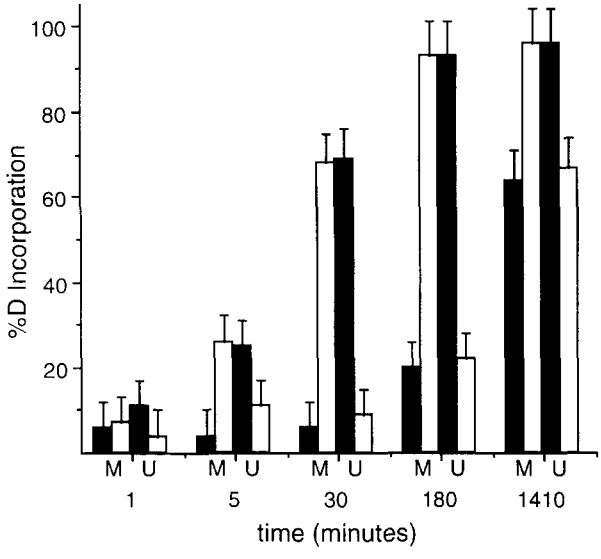

Fig. 3. Region in hydrophobic pocket that is destabilized by calcium ions when recoverin is N-acylated, yet is stabilized by calcium ions when recoverin is not acylated. Bar plots showing deuterium incorporation after incubation in buffered D_2O (pD 7.4) for various times for a region of myristoylated (M) and unmodified (U) recoverin encompassing residues 85–89 in the absence (black bars) and presence (white bars) of Ca^{2+}. This segment of recoverin includes Tyr 85 and Val 86, which were shown by NMR (Tanaka et al., 1995) to be within 5 Å of the acyl group in the NMR structure of calcium-bound myristoylated recoverin.

results were obtained for the peptide containing residues 90–104. Otherwise, N-lauroylated recoverin exhibited similar rates of HDX as the N-myristoylated protein. Hereafter, use of the term "N-acylated" will imply similar behavior for both N-lauroylated and N-myristoylated recoverin, except for those quantitative differences observed in regions 85–89 and 90–104.

A summary of the effects of Ca^{2+} binding and fatty acylation of recoverin on deuterium exchange rates is presented in Tables 1 and 2 and Figure 5. Table 1 shows some of the changes in exchange rates for regions of recoverin that were derived from peptic digestion of the N-myristoylated and the unacylated protein (plus or minus Ca^{2+}). Likewise, Table 2 lists a few of the exchange rate changes (or lack of change) observed when comparing N-myristoylated and N-lauroylated recoverin. For acylated (N-myristoyl or N-lauroyl) recoverin (Fig. 5A), the binding of Ca^{2+} reduced HDX rates within the Ca^{2+}-binding EF hand 2 (peptic peptide 64–80) and EF hand 3 (peptic peptide 108–122), as well as an additional region in the C-terminal half of the protein (peptic peptide 130–157). Interestingly, HDX is reduced in the absence of Ca^{2+} in three regions (residues 31–35, 49–52, and 85–104) in the hydrophobic cleft that sequesters the myristoyl group when Ca^{2+} is absent (Tanaka et al., 1995). HDX is also reduced in a small helix (AA 181–184) (Ames et al., 1994) near the C-terminus. In contrast, no decrease in HDX rates was observed in the absence of Ca^{2+} for unmodified recoverin (Fig. 5B). Instead, several regions throughout unmodified recoverin demonstrated reduced HDX in the presence of Ca^{2+}.

To rule out nonspecific dication effects of Ca^{2+}, we repeated the isotopic exchange experiments described above in the presence of 2 mM Mg^{2+}. The inclusion of Mg^{2+} had no effect on the result of any of the experiments.

Discussion

The most reasonable interpretation of changes in HDX are in terms of solvent exclusion (Woodward et al., 1982) or stabilization of the associated hydrogen bonds within a protein (Englander & Kallenbach, 1984). For example, an earlier study found that a point mutation in the histidine-containing protein (HPr) from *Escherichia coli*, which resulted in a 1.5 kcal/mol stabilization over the wild-type protein, resulted in a reduction of the HDX rate within certain segments (Johnson, 1996). In contrast, a destabilizing point mutation resulted in a specific region of the protein exhibiting a faster HDX rate. Likewise, apo-myoglobin was found to have an increased rate of isotopic exchange compared to holo-myoglobin (Johnson & Walsh, 1994), where the latter is 5.5 kcal/mol more stable when comparing the differences in ΔG of folding (Griko et al., 1988). Thus, the concepts of solvent exclusion and/or stabilization of hydrogen bonds provide the framework for understanding and interpreting the results presented here for recoverin.

Previous evidence for the Ca^{2+}-myristoyl switch hypothesis was provided by proteolysis and membrane-binding studies (Zozulya & Stryer, 1992; Dizhoor et al., 1993), and by a comparison of the NMR structure of myristoylated calcium-free recoverin (Tanaka et al., 1995) with an X-ray structure of the unmyristoylated protein (N-myristoylated recoverin did not form suitable crystals) with a single calcium ion and one samarium ion bound (Flaherty et al., 1993). Ideally, one would want to compare N-acylated recoverin in the presence and absence of Ca^{2+}; however, it has not yet been possible to obtain a complete NMR-derived structure for calcium-bound acylated recoverin, because the protein tends to aggregate at higher concentrations. Lower protein concentrations were employed in the current mass spectrometric study, thereby circumventing this problem. Fluorescence and NMR studies have shown, however, that binding of Ca^{2+} results in extrusion of the acyl group into the solvent (Ames et al., 1995b; Hughes et al., 1995). Our results are consistent with this model and with the published structures, and they provide further evidence for the switch hypothesis by comparing directly the HDX rates of soluble acylated and nonacylated recoverin in both the presence and absence of Ca^{2+}.

Four regions of acylated recoverin exhibit a reduced isotopic exchange rate in the absence of Ca^{2+} (e.g., Figs. 3, 5; Table 1). Three of these sites are hydrophobic regions in the N-terminal half of acylated recoverin (residues 31–35, 49–52, and 85–104). Figure 6A depicts these three regions within the crystallographic structure of recoverin (Flaherty et al., 1993). Interestingly, the NMR structure for myristoylated recoverin shows that, in the absence of Ca^{2+}, these regions open to form a hydrophobic cleft into which the myristoyl group can be inserted, and each of these regions are in close contact with the myristoyl group (Tanaka et al., 1995). The reduction in exchange rate observed in the absence of Ca^{2+} is presumably due either to exclusion of solvent by the acyl group, which in this conformation is packed against the protein, or a stabilization of the hydrogen bonds in these regions via hydrophobic interactions between the acyl group and the hydrophobic side chains. In addition, a fourth hydrophobic region near the C-terminus of acylated recoverin was stabilized in the absence of Ca^{2+}. Because this region does not make direct contact with the N-terminal acyl group, it is interesting to speculate that this site may be sequestered in the Ca^{2+}-free conformation, but is exposed in the active Ca^{2+}-bound state and thus available for interaction with recoverin's effector molecule, rhodopsin kinase. Mutagenesis studies of this region should be able to test this hypothesis.

Table 1. *Hydrogen isotope exchange rate changes: Comparison of N-myristoylated and unmodified recoverin in the presence and absence of calcium*[a]

Position[b]	(M + Ca/M − Ca)[c]	(U + Ca/U − Ca)[d]	(M + Ca/U + Ca)[e]	(M − Ca/U − Ca)[f]
19–27	0.84	0.12	2.1	0.4
31–35	36	0.14	23	0.071
35–48	1.6	0.022	3.2	0.090
49–52	3.9	0.19	0.23	0.011
64–80	0.047	0.011	3.0	2.3
85–89	85	0.011	46	0.0061
90–104	19	0.53	0.69	0.017
108–122	0.23	0.0091	1.1	0.026
127–129	1.5	0.0035	0.53	0.0010
130–157	0.035	0.014	0.70	0.29
158–170	2.1	0.11	0.73	0.023
171–180	1.0	0.14	0.72	0.097
181–184	10	0.62	0.54	0.033

[a]Values indicate the ratios of the two deuterium exchange rates for the peptides resulting when the solution conditions (plus/minus Ca^{2+}) or covalent structure (myristoylated versus unmodified N-terminus) of recoverin is changed (see Materials and methods for an explanation of how these ratios were calculated).

[b]Residue numbering corresponds to that shown in Figure 5.

[c]Rate enhancement of N-myristoylated recoverin in the presence of 1 mM $CaCl_2$ over myristoylated recoverin in 1 mM EGTA (no Ca^{2+}).

[d]Rate enhancement of unmodified recoverin in the presence of 1 mM $CaCl_2$ over unmodified recoverin in 1 mM EGTA (no Ca^{2+}).

[e]Rate enhancement of myristoylated recoverin in the presence of 1 mM $CaCl_2$ over unmodified recoverin in 1 mM $CaCl_2$.

[f]Rate enhancement of myristoylated recoverin in the presence of 1 mM EGTA (no Ca^{2+}) over unmodified recoverin in 1 mM EGTA (no Ca^{2+}).

Whereas HDX rates decreased for the four hydrophobic regions in the absence of calcium (see above), segments encompassing two of the four EF-hands exhibited reductions in exchange rates in the presence of Ca^{2+} (see Figs. 2, 5; Table 1). These two EF-hands have sequences that would be expected to yield functional calcium-binding sites (EF-hands 2 and 3, corresponding to residues 73–84 and 109–120, respectively), and were also found to bind Ca^{2+} and Sm^{3+} in the crystal structure of nonacylated recoverin. Presumably, the reduction in HDX rates observed for these regions when Ca^{2+} is present is due to stabilization via metal chelation by the EF-hands. Regions that were stabilized in the presence of Ca^{2+} are depicted in the ribbon structure of Figure 6B. In contrast, EF-hands 1 and 4 (residues 35–47 and 159–170, respectively) have sequences that indicate that they are not functional and, in N-acylated recoverin, no changes in HDX rates were observed in these regions when Ca^{2+} was present.

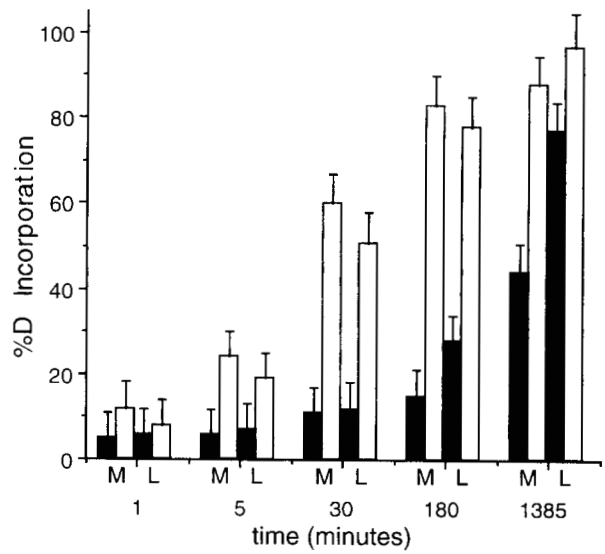

Fig. 4. Comparison of myristoylated (C14:0) and lauroylated (C12:0) recoverin. Bar plots showing deuterium incorporation after incubation in buffered D_2O (pD 7.4) for various times for regions of myristoylated (M) and lauroylated (L) recoverin encompassing residues 85–89 in the absence (black bars) and presence (white bars) of Ca^{2+}. In the absence of calcium, N-myristoylated recoverin exhibits a slightly reduced rate of HDX compared to the N-lauroylated protein.

Recoverin is one of four photoreceptor proteins known to be N-acylated by a family of fatty acids (Dizhoor et al., 1992; Kokame et al., 1992; Neubert et al., 1992; Johnson et al., 1994; Palczewski et al., 1994), and it was of interest to see if any differences in HDX rates could be discerned between myristoylated and lauroylated recoverin. The exchange rates for these two forms of recoverin were identical for nearly the entire protein. Exceptions include certain hydrophobic regions that exchange slowly in the absence of calcium—residues 85–89 (Fig. 4; Table 2) and 90–104 (Table 2). These data suggest that the shorter and less hydrophobic lauroyl group provides a reduced level of solvent exclusion or hydrophobic stabilization for these regions than myristic acid.

Many of the regions that did not seem to be affected by Ca^{2+} in the acylated protein were stabilized by Ca^{2+} in unmodified recoverin (Fig. 5; Table 1) and, in general, compared to the acylated protein, unmodified recoverin seemed to exhibit a decreased HDX rate in the presence of Ca^{2+}. We believe Ca^{2+} binding in these experiments has a greater stabilizing effect on nonacylated recov-

Table 2. *Hydrogen isotope exchange rate changes: Comparison of N-myristoylated and N-lauroylated recoverin in the presence and absence of calcium*[a]

Position[b]	(M + Ca/M − Ca)[c]	(L + Ca/L − Ca)[d]	(M + Ca/L + Ca)[e]	(M − Ca/L − Ca)[f]
31–35	36	38	0.64	0.63
49–52	3.9	3.9	0.44	0.46
85–89	85	13	1.5	0.31
90–104	19	11	0.45	036
181–184	10	8.0	0.90	0.70

[a]Values indicate ratios of the two deuterium exchange rates for the peptides resulting when the solution conditions (plus/minus Ca^{2+}) or covalent structure (myristoylated versus lauroylated N-terminus) of recoverin is changed (see Materials and methods for an explanation of how these ratios were calculated).

[b]Residue numbering corresponds to that shown in Figure 5.

[c]Rate enhancement of N-myristoylated recoverin in the presence of 1 mM $CaCl_2$ over myristoylated recoverin in 1 mM EGTA (no Ca^{2+}).

[d]Rate enhancement of lauroylated recoverin in the presence of 1 mM $CaCl_2$ over lauroylated recoverin in 1 mM EGTA (no Ca^{2+}).

[e]Rate enhancement of myristoylated recoverin in the presence of 1 mM $CaCl_2$ over lauroylated recoverin in 1 mM $CaCl_2$.

[f]Rate enhancement of myristoylated recoverin in the presence of 1 mM EGTA (no Ca^{2+}) over lauroylated recoverin in 1 mM EGTA (no Ca^{2+}).

erin because acylated recoverin must extend the acyl group into aqueous buffer, a process that is unfavorable energetically. In this way, the acylated N-terminus of recoverin may be "communicating" (in the reverse direction) structural instability to the Ca^{2+}-binding regions along the same pathway that enables Ca^{2+} binding to facilitate the extrusion of the acyl group from the hydrophobic pocket.

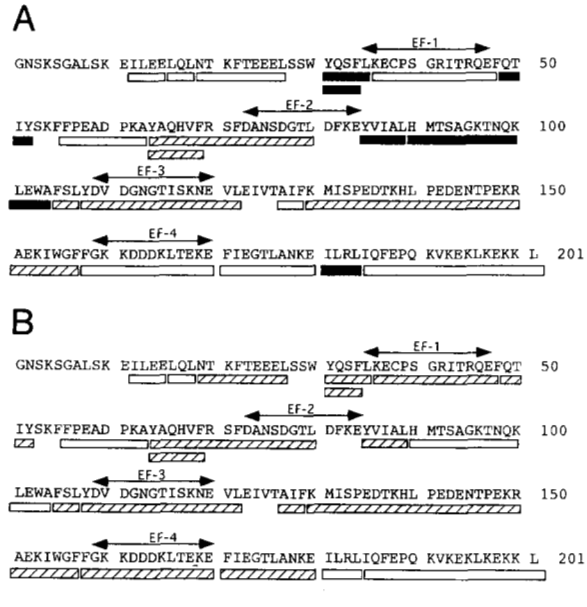

Fig. 5. Summary of changes in HDX observed for (**A**) N-acylated (myristoylated or lauroylated) and (**B**) unmodified recoverin. Bars beneath the sequences indicate peptic peptides identified by tandem mass spectrometry. Open bars signify regions delineated by peptic cleavage that exhibited no change in exchange rates. Hatched bars indicate regions where there was a reduction in exchange rate in the presence of Ca^{2+}; in contrast, solid bars denote regions where there was a reduction in exchange rate in the absence of Ca^{2+}. The four EF-hands are indicated above the sequences by the double-headed arrows. From the sequence, only EF-2 and EF-3 are expected to bind calcium.

The increased HDX rate of unmodified protein in the absence of Ca^{2+} suggests that this form of recoverin may be transiently unfolded, i.e., possess a less stable structure than acylated recoverin. This is consistent with this form of recoverin being more susceptible to proteolysis than the acylated or Ca^{2+}-bound protein (Dizhoor et al., 1993). CD studies (Kataoka et al., 1993) indicate that the α-helical character of nonacylated recoverin is similar to that of acylated recoverin, and NMR data (Ames et al., 1995b) suggest similar structures for Ca^{2+}-bound myristoylated and nonmyristoylated recoverin. These results indicate that the acylation-dependent changes in HDX rates that we observe are due to differences in protein dynamics rather than to large changes in protein structure.

On the other hand, from calcium-binding studies, it was proposed that recoverin exists in two conformational states referred to as T and R (Ames et al., 1995a). In the R state, Ca^{2+} binds more tightly than the T state and has two dissociation constants of 0.11 and 6.9 μM. It was estimated that, for unliganded myristoylated recoverin, the ratio T/R is 400, but this changes to less than 0.05 for nonacylated recoverin. It was therefore hypothesized that the N-acyl group serves two functions: as a membrane anchor, and to shift the T/R conformational ratio by 8,000-fold. The large differences in HDX rates described here for acylated and unmodified recoverin (Table 1) are also consistent with the idea that the N-acyl group is important for maintaining a specific conformation. Taken together, the data suggest that, rather than acting as a simple lever that moves to and from a hydrophobic patch of recoverin, the N-acyl group exerts a significant influence on the conformation and/or dynamics of several regions of the protein.

We were unable to compare deuterium exchange rates for the N-terminal region (Gly 1–Glu 11), because deuterium exchange appeared to proceed to completion in all forms of recoverin within the first minute, our earliest measured point. Furthermore, the mass spectral signal intensity for this peptide was low, and the data were inconclusive.

Using the new technique of monitoring hydrogen isotope exchange by ESI/MS, we have obtained structural information that is consistent with and adds to information gained by other biochemical and biophysical methods employed to study the calcium-

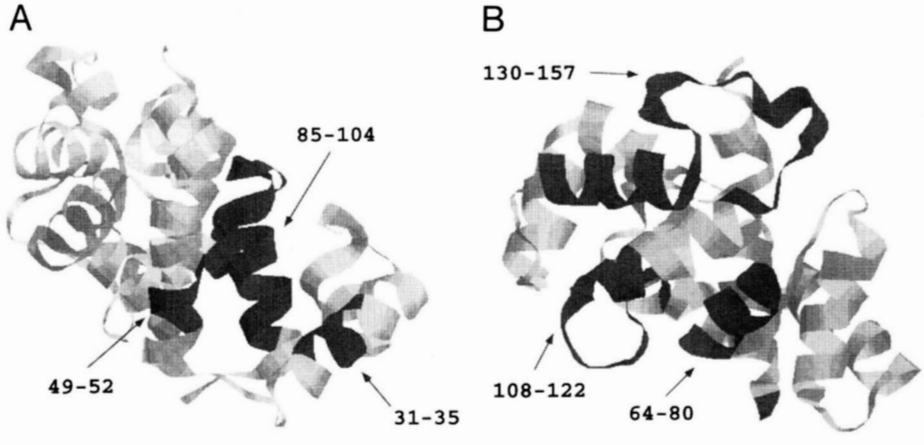

Fig. 6. A: Ribbon diagram of recoverin showing three regions where there was a reduction in isotopic exchange rates in the absence of Ca^{2+} (residues 31–35, 49–52, and 85–104). **B:** Ribbon diagram of recoverin showing three regions where there was a reduction in isotopic exchange rates in the presence of Ca^{2+}. The orientation of the diagram in B is approximately a 90° rotation to the right compared to the diagram in A.

myristoyl switch of recoverin. Although the structural information gained by this method is of lower resolution than that obtained by NMR or X-ray crystallography, it does not suffer from many of the limitations of these techniques. In principal, there are no size limitations (except for increased complexity of analysis), and it is possible to use small amounts of material, under more physiological conditions. We have examined the influence of a posttranslational modification (N-acylation), as well as the effect of ligand binding (Ca^{2+}) on the conformation of recoverin. The significant effect of N-acylation on the conformation and/or dynamics of recoverin was revealed, and our ability to compare directly different forms of recoverin in both the presence and absence of Ca^{2+} aids in the interpretation of the two disparate structures obtained by two different techniques (Flaherty et al., 1993; Tanaka et al., 1995). Because the relatively new technique used by us yielded results consistent with those obtained by the more established techniques of X-ray crystallography and NMR, we believe mass spectrometric measurement of hydrogen isotope exchange may also be useful for examining intermolecular reactions that presently cannot be examined by other methods, for example, between recoverin and rhodopsin kinase.

Materials and methods

Preparation of recoverin

Recoverin was expressed in *E. coli* strain BL21(DE3) containing plasmids encoding for recoverin (pET11a-mr21) and *N*-myristoyltransferase (pBB 131) as described (Ray et al., 1992). The *E. coli* were grown at 37 °C with shaking in Luria-Bertoni medium containing 100 μg/mL kanamycin and 100 μg/mL ampicillin. When the *E. coli* reached an OD_{660} of 0.3 absorbance units, 100 μg/mL (final concentration) C12:0 or C14:0 free fatty acid was added from 100 mg/mL ethanol stock solutions. The plasmids were induced 20 min later by the addition of 0.5 mM (final concentration) isopropyl β-D-thiogalactoside. The bacteria were harvested 2 h after induction by centrifugation in a Sorvall GSA rotor for 20 min at 4,000 RPM. After centrifugation, the bacterial pellets were frozen at −80 °C. The cell pellets were thawed by resuspending in buffer A (100 mM Tris, pH 8.0, 50 mM NaCl, 2 mM $MgCl_2$, 1 mM DTT, 200 μM $CaCl_2$, and 5% glycerol) at a density of 15 mL buffer/bacteria from 1 L culture. The cells were lysed by sonicating 5 times for 2 min on ice with a Branson sonicator using a 1-cm probe, 50% duty cycle, and 70% power. The lysates were centrifuged at 25,000 RPM for 45 min in a Sorvall SW-27 rotor at 4 °C. Additional $CaCl_2$ (200 μM) was added to the supernatant fluid, which was then applied to a 40-mL phenyl-Sepharose CL-4B (Pharmacia) column that had been equilibrated in buffer A at 4 °C. After washing the column with 5 column volumes of buffer A, the recoverin was eluted with 5 column volumes of buffer B (5 mM EGTA in buffer A). The eluate, containing recoverin, was concentrated by filtration using a YM 10 filter (Amicon) to a volume of 10 mL, then applied to a preparative (30 × 300 mm) C18 reverse-phase column (Waters) to separate unmodified recoverin from recoverin modified by C12:0 and C14:0. The recoverin was eluted with a gradient containing 0–70% acetonitrile in 0.1% TFA at a flow rate of 35 mL/min. The recoverin purified in this manner was presumably denatured because it bound irreversibly to a phenyl-Sepharose column, even after transfer to aqueous buffer at neutral pH. However, it could be renatured in the following manner. Fractions containing recoverin were dried by lyophilization, redissolved in 2 mL 8 M urea, and diluted dropwise in 2 L of buffer containing 100 mM Tris, pH 8.0, and 1 mM EGTA at 20 °C. The resulting renatured recoverin was again purified by phenyl-Sepharose chromatography as described.

Of the recoverin produced by *E. coli* incubated with C12:0 free fatty acid, HPLC and ESI/MS analysis showed that approximately 55% was unmodified, 35% was modified by C12:0, and the remaining 10% was modified by C14:0, which presumably was derived from endogenous pools of myristoyl CoA within *E. coli*. After preparative HPLC, each form of recoverin was more than 95% pure as monitored by ESI/MS. After renaturation and phenyl-Sepharose chromatography, the recombinant recoverin was in an active, native-like conformation based on the following criteria. (1) The renatured recoverin bound to phenyl-Sepharose in a Ca^{2+}-dependent manner. (2) In a native gel electrophoresis system (Teng et al., 1994), both calcium-bound and calcium-free renatured recombinant recoverin comigrated with recoverin that had not been denatured by reverse-phase HPLC. (3) The renatured recoverin was able to inhibit rhodopsin kinase activity in a calcium-dependent manner (assay conditions described by Chen et al., 1995) with the

same specific activity as nondenatured recoverin. Approximately 90% of the recoverin activity and mass were recovered after reverse-phase HPLC and renaturation.

HDX

HDX experiments were performed on three forms of recoverin: the unmodified protein, plus two that had been N-terminally acylated with either C12:0 or C14:0. Exchange rates were measured for all three forms in both the presence and absence of calcium, resulting in a total of six different experimental conditions. Lyophilized recoverin (115 μg, 5 nmol) was first solubilized at room temperature for 15 min in 40 μL of 200 mM, pH 7.0, Tris buffer in H_2O containing either 20 mM $CaCl_2$ (buffer 1A) or 20 mM EGTA (buffer 1B). Deuterium exchange was performed at room temperature and was initiated by the addition of 760 μL D_2O containing 20 mM β-mercaptoethanol and 100 mM KCl to the solubilized protein. The measured pD (no isotopic correction) was 7.4. Aliquots of 40 μL were quenched at various times by the addition of 40 μL of 500 mM, pH 2.6, potassium phosphate in water (buffer 2). Quenched samples were immediately frozen in liquid nitrogen and stored at -70 °C until analyzed by LC/MS. The peptides could be stored for at least one week under these conditions with no observable loss of deuterium label. An additional set of experiments was performed in which the dried proteins were first dissolved in 200 mM Tris, pH 7.0, with 40 mM $MgCl_2$ and containing either 20 mM $CaCl_2$ or 20 mM EGTA. These experiments, performed in the presence of Mg^{2+}, yielded results identical to those without.

The actual number of deuteriums incorporated into peptides (percent deuterium incorporation) was calculated by comparison with two controls: a zero time point and the completely deuterated protein. The zero time point was obtained by dissolving 5 nmol recoverin in 40 μL of buffer 1A, and adding D_2O (760 μL) acidified previously with 800 μL buffer 2. Aliquots of 80 μL were frozen. In previous experiments (Johnson & Walsh, 1994), the fully deuterated control was produced by boiling the protein in neutral pD D_2O. With such treatment, however, recoverin forms an insoluble aggregate. To obtain this control, recoverin was digested first with pepsin, lyophilized, and the fragments were boiled at neutral pD. The percent incorporation of deuterium was calculated as follows (Zhang & Smith, 1993):

$$D\% = (m_t - m_{0\%})/(m_{100\%} - m_{0\%}) \times 100,$$

where m_t is the peptide (or protein) mass at time t, $m_{0\%}$ is the mass of the peptide at time zero, and $m_{100\%}$ is the peptide mass at infinite time (completely deuterated). From the fully deuterated controls, it was found that peptides typically lose about 45% of their deuterium label during the LC/MS analysis. For peptides that exhibited ions of multiple charge states, the mass measurement errors were assumed to be the standard deviation of the set of molecular weight measurements derived from each charge state. Peptides represented by only a single ion were assumed to have an error of ± 0.15 Da. It is important to note that, for each time point, LC/MS data were obtained sequentially for the six experimental conditions (i.e., unmodified recoverin with and without calcium, C14:0-modified recoverin with and without calcium, and C12:0-modified recoverin with and without calcium). Of key interest in this study were the differences in molecular weights obtained under the different experimental conditions, and not the precise value of the percent deuterium incorporation. For this reason, the errors in measurement of $m_{0\%}$ and $m_{100\%}$ (equation above) were not propagated, and only the error associated with m_t was used to derive the error bars.

Data (percentage of unexchanged hydrogens versus the time in minutes after addition of D_2O) were fit to the sum of up to three exponentials using the computer program Sigma Plot; i.e., $y = A(e^{-at}) + B(e^{-bt}) + C(e^{-ct})$, where y is the percentage of unexchanged hydrogen remaining; t is the time in minutes after addition of D_2O; a, b, and c are three independent rate constants; and A, B, and C are the percentages of exchangeable hydrogens with exchange rate constants of a, b, and c, respectively. In many cases, fitting the data to the sum of three exponentials resulted in considerable dependencies between parameters, indicating that fewer exponentials would suffice. In these situations, the data were fit to the sum of two exponentials, or in some cases, a single exponential. Values for A, B, C, a, b, and c appear in the Electronic Appendix.

The values in Tables 1 and 2 indicate the relationship between the deuterium exchange rates of each peptic peptide for each experimental condition. For example, in the column labeled (M + Ca/M − Ca), data obtained from myristoylated recoverin in the presence of calcium were fit to a curve obtained for the same peptide in the absence of calcium by determining the factor g in the equation $y = A(e^{-agt}) + B(e^{-bgt}) + C(e^{-cgt})$, where values of A, B, C, a, b, and c were obtained from the same peptide in the absence of calcium. Likewise, data for the peptide in the absence of calcium were fit to the same equation where the parameters A, B, C, a, b, and c describe the curve for that peptide in the presence of calcium. The values in Tables 1 and 2 represent the average of the two values of the factor g obtained in this manner. We take this average value to approximate the ratio of the deuterium exchange rates for a given peptide under different experimental conditions.

LC/MS

LC/MS was performed with an API-III triple quadrupole mass spectrometer (PESciex, Foster City, California) equipped with a nebulization-assisted electrospray ionization source. An Applied Biosystems, Inc. (ABI) syringe pump (model 140A) was used to generate 15-min HPLC gradients of 0–60% acetonitrile containing 0.02% trifluoroacetic acid, pH 2.8, at 75 μL/min through a 1 × 30-mm C_8 column. Solvent was directed through a coil of narrow bore stainless steel tubing that was immersed in an ice bath prior to a Rheodyne injector and the column. A post column splitting tee was used to divert approximately two-thirds of the effluent to an ABI model 785A UV detector, with the remainder directed toward the mass spectrometer. Mass spectra were acquired using a step size of 0.2 Da, with a dwell time of 1 ms at unit resolution.

Partially deuterated samples were removed individually from the freezer, thawed, and proteolyzed immediately by the addition of pepsin with an enzyme to substrate ratio of 1:1 by weight. After 5 min of peptic digestion on ice, the sample was injected onto the C_8 column, and the acetonitrile gradient started after 5 min of desalting. The column was disconnected from the mass spectrometer for the duration of the desalting period, and reconnected prior to initiation of the acetonitrile gradient. The molecular weights of partially deuterated peptides were determined by calculation of centroids of the peak envelope.

Peptic peptides were identified using tandem mass spectrometry (Hunt et al., 1986; Biemann, 1990) with a step of 0.25 Da and a

dwell time of 1 ms. Resolution in the first and third quadrupoles was sufficient to transmit a window of width 2–3 Da. Precursor ions were accelerated to kinetic energies ranging from 15 to 25 eV and activated collisionally with argon in the second quadrupole. The instrument control software reports the collision gas pressure as a "gas thickness," which was typically set to 2.5×10^{14} atoms of argon/cm^3. Tandem mass spectral data interpretation was accomplished using software written in-house (Taylor et al., 1996).

Supplementary material in Electronic Appendix

Four tables are included in the Electronic Appendix. Table I contains hydrogen isotopic exchange rates and the percentage of amides associated with each exchange rate for peptic peptides obtained from myristoylated recoverin. Table II contains hydrogen isotopic exchange rates and the percentage of amides associated with each exchange rate for peptic peptides obtained from unmodified recoverin. Table III contains hydrogen isotopic exchange rates and the percentage of amides associated with each exchange rate for peptic peptides obtained from lauroylated recoverin. Table IV contains the percentage of amide hydrogens that were back-exchanged during analysis for each peptic peptide.

Acknowledgments

We thank Jason Chen for help and advice in expressing and purifying recoverin and for advice on assaying its activity. We also thank Lubert Stryer and Jim Ames for sharing unpublished data and for helpful discussions. This work was supported by National Institutes of Health NRSA grant 5F32-EYO6450-02 (T.A.N.), the University of Washington Royalty Research Fund (R.S.J), and NIH grant EY06641 (J.B.H.).

References

Ames JB, Porumb T, Tanaka T, Ikura M, Stryer L. 1995a. Amino-terminal myristoylation induces cooperative calcium binding to recoverin. *J Biol Chem 270*:4526–4533.

Ames JB, Tanaka T, Ikura M, Stryer L. 1995b. Nuclear magnetic resonance evidence for calcium-induced extrusion of the myristoyl group of recoverin. *J Biol Chem 270*:30909–30913.

Ames JB, Tanaka T, Stryer L, Ikura M. 1994. Secondary structure of myristoylated recoverin determined by three-dimensional heteronuclear NMR: Implications for the calcium-myristoyl switch. *Biochemistry 33*:10743–10753.

Biemann K. 1990. Sequencing of peptides by tandem mass spectrometry and high-energy collision-induced dissociation. *Methods Enzymol 193*:455–479.

Chen CK, Inglese J, Lefkowitz RJ, Hurley JB. 1995. Ca++ dependent interaction of recoverin with rhodopsin kinase. *J Biol Chem 270*:18060–18066.

Covey TR, Huang EC, Henion JD. 1991. Structural characterization of protein tryptic peptides via liquid chromatography/mass spectrometry and collision-induced dissociation of their doubly charged molecular ions. *Anal Chem 63*:1193–1200.

Dizhoor AM, Chen CK, Olshevskaya E, Sinelnikova VV, Phillipov P, Hurley JB. 1993. Role of the acylated amino terminus of recoverin in calcium-dependent membrane interaction. *Science 259*:829–832.

Dizhoor AM, Ericsson LH, Johnson RS, Kumar S, Olshevskaya E, Zozulya S, Neubert TA, Stryer L, Hurley JB, Walsh KA. 1992. The NH_2 terminus of retinal recoverin is acylated by a small family of fatty acids. *J Biol Chem 267*:16033–16036.

Englander SW, Kallenbach NR. 1984. Hydrogen exchange and structural dynamics of proteins and nucleic acids. *Quart Rev Biophys 16*:521–655.

Fenn JB, Mann M, Meng CK, Wong SF, Whitehouse CM. 1989. Electrospray ionization for mass spectrometry of large biomolecules. *Science 246*:64–71.

Flaherty KM, Zozulya S, Stryer L, McKay DB. 1993. Three-dimensional structure of recoverin, a calcium sensor in vision. *Cell 75*:709–716.

Gray-Keller MP, Polans AS, Palczewski K, Detwiler PB. 1993. The effect of recoverin-like calcium-binding proteins on the photoresponse of retinal rods. *Neuron 10*:523–531.

Griko YV, Privalov PL, Venyaminov SY, Kutyshenko VP. 1988. Thermodynamic study of apomyoglobin structure. *J Mol Biol 202*:127–138.

Hughes RE, Brzovic PS, Klevit RE, Hurley JB. 1995. Calcium-dependent solvation of the myristoyl group of recoverin. *Biochemistry 34*:11410–11416.

Hunt DF, Yates JR, Shabanowitz J, Winston S, Hauer CR. 1986. Protein sequencing by tandem mass spectrometry. *Proc Natl Acad Sci USA 83*:6233–6237.

Johnson RS. 1996. Mass spectrometric measurements of changes in protein hydrogen exchange rates resulting from point mutations. *J Am Soc Mass Spectrom 7*:515–521.

Johnson RS, Ohguro H, Palczewski K, Hurley JB, Walsh KA, Neubert TA. 1994. Heterogeneous N-acylation is a tissue- and species-specific posttranslational modification. *J Biol Chem 269*:21067–21071.

Johnson RS, Walsh KA. 1994. Mass spectrometric measurement of protein amide hydrogen exchange rates of apo- and holo-myoglobin. *Protein Sci 3*:2411–2418.

Kataoka M, Mihara K, Tokunaga F. 1993. Recoverin alters its surface properties depending on both calcium-binding and N-terminal myristoylation. *J Biochem (Tokyo) 114*:535–540.

Katta V, Chait BT. 1993. Hydrogen/deuterium exchange electrospray ionization mass spectrometry: A method for probing protein conformational changes in solution. *J Am Chem Soc 115*:6317–6321.

Kawamura S. 1993. Rhodopsin phosphorylation as a mechanism of cyclic GMP phosphodiesterase regulation by S-modulin. *Nature 362*:855–857.

Kokame K, Fukada Y, Yoshizawa T, Takao T, Shimonishi Y. 1992. Novel lipid modification at the N-terminus of photoreceptor G protein alpha-subunit. *Nature 359*:749–752.

Liu Y, Smith DL. 1994. Probing high order structure of proteins by fast-atom bombardment mass spectrometry. *J Am Soc Mass Spectrom 5*:19–28.

Moncrief ND, Kretsinger RH, Goodman M. 1990. Evolution of EF-hand calcium-modulated proteins. I. Relationships based on amino acid sequences. *J Mol Evol 30*:522–562.

Neubert TA, Johnson RS, Hurley JB, Walsh KA. 1992. The rod transducin alpha subunit amino terminus is heterogeneously fatty acylated. *J Biol Chem 267*:18274–18277.

Palczewski K, Subbaraya I, Gorczyca WA, Helekar BS, Ruiz CC, Ohguro H, Huang J, Zhao X, Crabb JW, Johnson RS, Walsh KA, Gray-Keller MP, Detwiler PB, Baehr W. 1994. Molecular cloning and characterization of retinal photoreceptor guanylyl cyclase activating protein (GCAP). *Neuron 13*:395–404.

Ray S, Zozulya S, Niemi GA, Flaherty KM, Brolley D, Dizhoor AM, McKay DB, Hurley J, Stryer L. 1992. Cloning, expression, and crystallization of recoverin, a calcium sensor in vision. *Proc Natl Acad Sci USA 89*:5705–5709.

Sanada K, Kokame K, Yoshizawa T, Takao T, Shimonishi Y, Fukada Y. 1995. Role of heterogeneous N-terminal acylation of recoverin in rhodopsin phosphorylation. *J Biol Chem 270*:15459–15462.

Tanaka T, Ames JB, Harvey TS, Stryer L, Ikura M. 1995. Sequestration of the membrane-targeting myristoyl group of recoverin in the calcium-free state. *Nature 376*:444–446.

Taylor JA, Walsh KA, Johnson RS. 1996. Sherpa: A Macintosh based expert system for the interpretation of ESI LC/MS and MS/MS of protein digests. *Rapid Commun Mass Spectrom 10*:679–687.

Teng DH, Chen CK, Hurley JB. 1994. A highly conserved homologue of bovine neurocalcin in *Drosophila melanogaster* is a Ca++ binding protein expressed in neuronal tissues. *J Biol Chem 269*:31900–31907.

Woodward C, Simon I, Tuchsen E. 1982. Hydrogen exchange and the dynamic structure of proteins. *Mol Cell Biochem 48*:135–160.

Zhang Z, Post CB, Smith DL. 1996. Amide hydrogen exchange determined by mass spectrometry: Application to rabbit muscle aldolase. *Biochemistry 35*:779–791.

Zhang Z, Smith DL. 1993. Determination of amide hydrogen exchange by mass spectrometry: A new tool for protein structure elucidation. *Protein Sci 2*:522–531.

Zozulya S, Stryer L. 1992. Calcium-myristoyl protein switch. *Proc Natl Acad Sci USA 89*:11569–11573.